Environment International 140 (2020) 105763

Contents lists available at ScienceDirect

Environment International

journal homepage: www.elsevier.com/locate/envint

Gut microbiota perturbations and neurodevelopmental impacts in offspring rats concurrently exposure to inorganic arsenic and fluoride

Yulan Qiu[a,1], Xushen Chen[b,1], Xiaoyan Yan[a], Jie Wang[c,d], Guan Yu[e], Wenyan Ma[a], Bo Xiao[f], Sarah Quinones[b], Xiaolin Tian[g], Xuefeng Ren[b,f,*]

[a] School of Public Health, Shanxi Medical University, Taiyuan, Shanxi, PR China
[b] Department of Epidemiology and Environmental Health, School of Public Health and Health Professions, University at Buffalo, Buffalo, NY, USA
[c] Department of Biochemistry, Jacobs School of Medicine and Biomedical Sciences, University at Buffalo, Buffalo, NY, USA
[d] Department of Biostatistics and Bioinformatics, Roswell Park Comprehensive Cancer Center, Buffalo, NY, USA
[e] Department of Biostatistics, School of Public Health and Health Professions, University at Buffalo, Buffalo, NY, USA
[f] Department of Pharmacology and Toxicology, Jacobs School of Medicine and Biomedical Sciences, University at Buffalo, Buffalo, NY, USA
[g] Shanxi Key Laboratory of Experimental Animal and Human Disease Animal Models, Shanxi Medical University, Taiyuan, Shanxi, PR China

ARTICLE INFO

Handling Editor: Yong-Guan Zhu

Keywords:
Inorganic arsenic
Fluoride
Concurrent exposure
Gut microbiota perturbations
Neurodevelopmental impacts

ABSTRACT

Many "hot spot" geographic areas across the world with drinking water co-contaminated with inorganic arsenic (iAs) and fluoride (F^-), two of the most common natural contaminants in drinking water. Both iAs and F^- are known neurotoxins and affect neurodevelopment of children. However, very few studies have investigated the neurodevelopmental effects of concurrent exposure to iAs and F^-, which could potentially pose a greater risk than iAs or F^- exposure alone. Further, perturbations of gut microbiota, which plays a regulatory role in neurodevelopment, resulting from iAs and F^- exposure has been reported in numerous studies. There is lacking of information regarding to the relationship among concurrent iAs and F^- exposure, microbiome disruption, and neurodevelopmental impacts. To fill these gaps, we treated offspring rats to iAs (50 mg/L $NaAsO_2$) and F^- (100 mg/L NaF), alone or combined from early life (*in utero* and childhood) to puberty. We applied Morris water maze test to assess spatial learning and memory of these rats and generated gut microbiome profiles using 16S rRNA gene sequencing. We showed that concurrent iAs and F^- exposure caused more prominent neurodevelopmental effects in rats than either iAs or F^- exposure alone. Moreover, Unsupervised Principal Coordinates Analysis (PCoA) and Linear Discriminant Analysis Effect Size (LEfSe) analysis of gut microbiome sequencing results separated concurrent exposure group from others, indicating a more sophisticated change of gut microbial communities occurred under the concurrent exposure condition. Further, a correlation analysis between indices of the water maze test and microbial composition at the genus level identified featured genera that were clearly associated with neurobehavioral performance of rats. 75% (9 out of 12) genera, which had a remarkable difference in relative abundance between the control and combined iAs and F^- exposure groups, showed significantly strong correlations (r = 0.70–0.90) with the water maze performance indicators. Collectively, these results suggest that concurrent iAs and F^- exposure led to more prominent effects on neurodevelopment and gut microbiome composition structures in rats, and the strong correlation between them indicates a high potential for the development of novel microbiome-based biomarkers of iAs and/or F^- associated neurodevelopmental deficits.

1. Introduction

Inorganic arsenic (iAs) and fluoride (F^-) are two elements recognized as the most significant inorganic contaminants in drinking water worldwide (Thompson et al., 2007; Humans IWGotEoCRt, Some drinking-water disinfectants and contaminants, including arsenic IARC Monogr Eval Carcinog Risks Hum 84, 2004; Brouwer et al., 1988; Wen et al., 2013). Many geographic areas worldwide with drinking water have been found to be co-contaminated by iAs and F^-: in the US (Goldhaber et al., 1997; Levy et al., 1999), Latin America (e.g.,

* Corresponding author at: Department of Epidemiology and Environmental Health, School of Public Health and Health Professions, University at Buffalo, 3435 Main Street, Buffalo, New York 14214, USA.
E-mail address: xuefengr@buffalo.edu (X. Ren).
[1] These authors contributed equally.

https://doi.org/10.1016/j.envint.2020.105763
Received 13 November 2019; Received in revised form 14 March 2020; Accepted 22 April 2020
Available online 01 May 2020

Argentina, Bolivia, Chile, Colombia, Mexico, Peru) (Alarcon-Herrera et al., 2013; Buchhamer et al., 2012; Gonzalez-Horta et al., 2015; Rocha-Amador et al., 2007; Limon-Pacheco et al., 2018), Asia (e.g., China, India, Japan, Korea, Malaysia, Pakistan) (Chakraborti et al., 2011; Wang et al., 2007; Arshad and Imran, 2016), and Africa (Ethiopia, Ghana, Nigeria, Tanzania) (Amini et al., 2008; Bretzler et al., 2017; Merola et al., 2014; Obiri et al., 2016; Ogbu et al., 2012; Wambu et al., 2014).

Both iAs and F^- produce adverse effects on neurodevelopment and in turn deficits in neurobehavioral and cognitive function in children whose exposure occurred during pre- and post-natal periods (Wang et al., 2007; Tsai et al., 2003; Vibol et al., 2015; Rodriguez-Barranco et al., 2013; Borman and Fyfe, 2013; Das, 2016; Sebastian and Sunitha, 2015; Bashash et al., 2017; Grandjean and Landrigan, 2014). In recent decades, various epidemiological reports have shown that iAs exposure can alter neurobehavioral and cognitive function, particularly related to learning and memory, during childhood. Studies found a significant association between higher levels of urinary iAs concentrations and poor test scores measuring visual-spatial reasoning, language and vocabulary, memory and intelligence (Rosado et al., 2007), and hyperactive behavior (Roy et al., 2011) in children from Mexico. Similarly, a study conducted in India showed that children exposed to high levels of iAs in water throughout development and childhood performed poorly in vocabulary, math skills, memory, and overall cognition (von Ehrenstein et al., 2007). A *meta*-analysis concluded that iAs exposure was associated with a decrease in children's IQ (Rodriguez-Barranco et al., 2013). Extremely high levels of F^- are known to cause neurotoxicity in adults (Council, 2006). Negative impacts of F^- exposure on memory and learning have been also reported in rodent studies (Chioca et al., 2008). Strong evidence from a *meta*-analysis further confirmed that F^- adversely affects cognitive development in early life (Choi et al., 2012). However, considering large regions with drinking water co-contaminated by iAs and F^- and their potential synergistic neurotoxic effects, the study is lacking in assessing neurodevelopmental effects of iAs and F^- mixtures.

Numerous studies show that iAs and F^- exposure have a significant impact on gut and/or oral microbiome (Chi et al., 2016; Dheer et al., 2015; Isokpehi et al., 2014; Koopman et al., 2015; Lu et al., 2014; Chen et al., 2013; Reilly et al., 2016; Bisanz et al., 2014; Ghaisas et al., 2016; Yasuda et al., 2017; Luo et al., 2016). The gut microbiome has been recognized as a key regulator of neurodevelopment and behavior, and perturbations in the microbiome community could lead to developmental deficits in neurobehavioral and cognitive functions (Borre et al., 2014; Galland, 2014; Scheperjans et al., 2015; Mulle et al., 2013; De Angelis et al., 2013). Lu and colleagues were the first to investigate the impact of iAs exposure on gut microbiota composition and metabolic activity (Lu et al., 2014). Their study showed that arsenic exposure over 4 weeks significantly altered gut microbiota composition in mice. Interestingly, subsequent work suggested that arsenic mediated changes in murine gut microbiota composition and functional capacity may be sex specific (Chi et al., 2016). A recent study of a pregnancy cohort reported the associations between urinary iAs in 6-week-old infants and the early intestinal microbiome, both in terms of overall microbiome community composition and among bacterial taxa, which demonstrated a similar sex-specific effect (Hoen et al., 2018). Relatively few studies are available in terms of F^- exposure and the microbiome. A study suggested that F^- treatment appeared to have a selective effect on the composition of the oral, but not gut, microbial community in mice (Yasuda et al., 2017). But a study done in broiler chickens showed that high dietary F^- altered bacterial counts and the diversity and composition of gut microbiota (Luo et al., 2016). Similarly, another recent study suggested that excessive F^- intake could induce intestinal barrier damage in mice, leading to alterations in intestinal microflora (Liu et al., 2019).

While it is important to investigate the effects of iAs exposure alone and F^- alone, unraveling the relationship among concurrent iAs and F^- exposure, microbiome disruption and neurodevelopmental effects is not only scientifically important but also critical for public health practice in the development of novel biomarkers and cost-effectively preventive and therapeutic interventions. However, the relationship among these three aspects is less clearly understood. In the present study, we established a rat model in which offspring were exposed to relatively high-dose iAs and F^-, alone or in combination, from the early life (*in utero* and childhood) to puberty; evaluated their performance in spatial learning and memory *via* the Morris water maze test; investigated the alterations in gut microbiome community compositions and further examined the correlations between significantly different taxa and neurodevelopmental performance.

2. Materials and methods

2.1. Chemicals and reagents

Sodium fluoride (NaF) and sodium arsenite ($NaAsO_2$) were purchased from Sigma-Aldrich (St. Louis, MO, USA).

2.2. Animals and treatment

Healthy adult Sprague-Dawley rats (200–250 g) were provided by the Laboratory Animal Center of Shanxi Medical University (Taiyuan, China). Food and water were available *ad libitum* during the entire experimental period. The environmental condition of the animal house was maintained as 12:12 h day/night cycle, with a temperature of 24 ± 2 ℃. Ten days before mating, 4 male rats and 8 female rats were randomly divided into 4 groups: control group (Ck) receiving sterile water and exposure groups receiving 50 mg/L $NaAsO_2$ (As group), 100 mg/L NaF (F group) or combination of 50 mg/L $NaAsO_2$ and 100 mg/L NaF and (AsF concurrent group) in drinking water. Drinking water with chemicals was made fresh twice a week. After 10 days of exposure, the rats in corresponding groups were subject to mating in a 1:2 male-to-female ratio. Day 0 of pregnancy was confirmed once a vaginal plug indicating successful mating was established. Pregnant rats were continually exposed to relevant chemicals through drinking water until the 21st day after giving birth. Offspring rats were exposed to iAs and F^- through parental lactation during the 21-day lactation period; afterwards, 5 normal male offspring were randomly selected from each exposure group and provided with the same iAs and F^- treatment as their parents until postnatal day 90. Thus, while the main impact of iAs and F^- exposure came from early life, the influence of offspring could also from the short term exposure in parental rats. The selection rationale of iAs and/or F^- exposure concentration was described in our previous study (Tian et al., 2019). All experiments were performed in accordance with protocol approved by the Institutional Animal Care and Use Committee of Shanxi Medical University.

2.3. Morris water maze test

Following iAs and F^- exposure, rats were trained on the spatial reference memory version of the Morris water maze (RWD Life Science, Shenzhen, China) hidden platform task to evaluate their space navigation and spatial learning and memory. The circular water maze testing tank was 210 cm in diameter and was filled with water to a depth of 0.30 m, which was 2 cm higher than the escape platform of 0.28 m height and 10 × 10 cm. Non-toxic white paint was used to keep the water opaque, and the water was maintained at 24 ± 2 ℃. A variety of prominent visual maze cues were placed on the walls in the room. The platform was hidden in quadrant I during the space navigation training and removed at the time of space exploration task. The water maze test was divided into two sections: space navigation training (the first 5 days) and the space exploration task (day 6). In space navigation training, each rat was placed into each quadrant randomly in sequence and allowed to swim for a maximum of 120 s.

Remaining on the platform for no < 10 s was defined as a successful escape, and actual escape latency was recorded; otherwise, escape latency was recorded as 120 s and the corresponding rat was placed on platform for 10 s before the next training. The space navigation training was performed once a day at all four quadrants for 5 consecutive days. On the sixth day, the platform was removed, and each rat was placed in the water maze at the farthest point away from the platform. The latency to first reach the platform, the number of times crossing the platform and the residence time spent at target quadrant within the 120-seconds limit were recorded. The behaviors of rats in the water maze trial were recorded by a video tracking system equipped with an automatic analysis software SMARTV3.0 (Panlab, Harvard Apparatus, Barcelona, Spain).

2.4. Long-term potentiation (LTP) induced by high-frequency stimulation (HFS)

After the Morris water maze test, rats were anesthetized with 20% urethane (0.7 mL/kg, intraperitoneal injection) and placed on the stereotaxic apparatus (RWD Life Science, Shenzhen, China). The scalp over the bregma was exposed and ablated by H_2O_2 until the skull was visible. A small hole (3-mm diameter) was drilled in the skull at the position of 4.2 mm posterior to the bregma and 3.8 mm lateral to the midline. Then, rats were implanted with two epoxy insulated microelectrodes, a stimulating electrode in the lateral of hippocampus Schaffer region and a recording electrode in the stratum radiatum of the hippocampus CA1 region. Both electrodes were lowered slowly to the point where maximal field excitatory postsynaptic potential (fEPSP) was evoked by low frequency stimuli. After the position of the recording electrode was fixed, a 30-minute baseline fEPSP was recorded based on the stimulation inducing 40% amplitude of maximal fEPSP. After that, three trains of HFS (20 pulses at 200 Hz, with inter-train interval of 30 s) were used to induce LTP. fEPSP was recorded in a 60-minute period at 1-minute intervals. The fEPSP at a specific minute was calculated by averaging two values recorded in that period. Each fEPSP was normalized to the baseline fEPSP. The data from 1 min, 30 min and 60 min were utilized as representative points to reflect LTP amplitude in the 60-minute window.

2.5. Hematoxylin and eosin (H&E) staining of hippocampus

The brain tissues of rats were harvested and fixed in 4% paraformaldehyde for 24 h at room temperature. The brains were rinsed in distilled water for 10 min before being dehydrated through serial ethanol baths (80%, 90%, 95%, 100%) for 2 h each, then cleaned in xylene and embedded in paraffin. Coronal sections were cut using a microtome at 4-μm thickness. Sections were mounted on glass slides, then stained with hematoxylin and eosin according to the technique previously reported (Bancroft and Gamble, 2008). Slides were mounted with neutral mounting medium and photographed using an inverted microscope (Zeiss Axio Observer, ZEISS, Jena, Germany).

2.6. Fecal sample collection, DNA extraction and 16S rRNA gene sequencing

Fecal pellets from individual rat selected for this experiment were collected at postnatal day 90 for 16S rRNA analysis, and stored in liquid nitrogen before being transferred to −80 °C refrigeration until further analysis. Fecal DNA was extracted using the QIAamp® DNA Stool Mini Kit (Qiagen, Hilden, Germany) according to the manufacturer's instructions. Quantification of DNA was performed using a NanoDrop One spectrophotometer (Thermo Fisher Scientific, Fitchburg, WI), and the integrity and size were assessed by 0.8% agarose gel electrophoresis. Isolated DNA was used to amplify the 16S rRNA gene of bacteria using the universal primers set 338F (5′-ACTCCTACGGGAGGCAGCA-3′) and 806R (5′-GGACTACHVGGGTWTCTAAT-3′), targeting the hypervariable regions V3-V4 of bacterial 16S rRNA. PCR amplification, preparation of sequencing library and pyrosequencing were performed on the Illumina MiSeq platform by Personal Biotechnology, Co., Ltd. (Shanghai, China).

2.7. Bioinformatics data analysis

The 16S rRNA raw sequencing data were processed using the open-source software QIIME 2 (version: 2019.1) (Bolyen et al., 2019). Sequences were demultiplexed and V3/V4 primer were removed using cutadapt (v2.8). The DADA2 plugin package was utilized for amplicon workflow: quality filtering, sequence truncation, denoise (error correction), sample inference, merging of paired-end reads, chimera identification and removal, singletons removal, dereplication of sequences into operational taxonomic unit (OTU) with 100% sequence similarity (Callahan et al., 2016). OTUs with a frequency of < 0.1% of the total number of reads were discarded. Taxonomic classification was conducted with a Naive-Bayes classifier trained against the SILVA 132 database (Quast et al., 2012) targeted for V3/V4 region of the 16S rRNA. Alpha and beta diversity metrics were calculated in QIIME 2 (version: 2019.1). Alpha diversity indices of Abundance-based Coverage Estimator (ACE), Chao1 and Shannon were estimated based on rarefied sequence count. Beta diversity analysis was performed using unsupervised principal coordinates analysis (PCoA) of Bray-Curtis dissimilarity to illustrate differences of microbiome composition profiles at OTU level. Linear discriminant analysis effect size (LEfSe) analysis (Segata et al., 2011) was employed to identify distinguishing taxa among the iAs and/or F^- exposure groups and control group at multiple levels and to visualize the results using cladogram and bar plot. The correlation matrix between microbiome composition and water maze performance was generated using Pearson's correlation coefficient. A heat map of this correlation matrix was created using the online platform Morpheus (https://software.broadinstitute.org/morpheus).

2.8. Statistical analysis

All statistical analyses were performed using SPSS 22.0 software (IBM, Chicago, IL, USA). The results of all the measurements are presented as the mean ± SEM. The differences between groups were evaluated by one-way analysis of variance (ANOVA) followed by pairwise comparisons. A P-value < 0.05 was considered statistically significant.

3. Results

3.1. Effects of iAs, F^-, alone or in combination, on spatial learning and memory of rats

The influences of iAs and F^-, alone or in combination, on spatial learning and memory of rats were evaluated using the Morris water maze test, consisting of space navigation training and space exploration task. As shown in Fig. 1A, on the first day of space navigation training, rats in groups other than AsF combination group took the longest amount of time to find the platform during 5-day training period. Except for the AsF combination group, a time dependent decrease of escape latency was observed along the training days. From the second training day, rats in the control group showed consistently shorter latency in locating the hidden platform. The escape latency of rats in the AsF combination group was significantly longer than any other group on the third training day. Additionally, another remarkable difference was noted between the control group and the AsF combination group on the fifth training day. No other statistically significant differences were observed. The representative trajectories (Fig. 1E) taken by rats at the last training day showed longer escape latency in the iAs and/or F^- exposure group compared with the control group. Rats in the F^- alone and AsF combination groups moved more along the wall of the pool. In

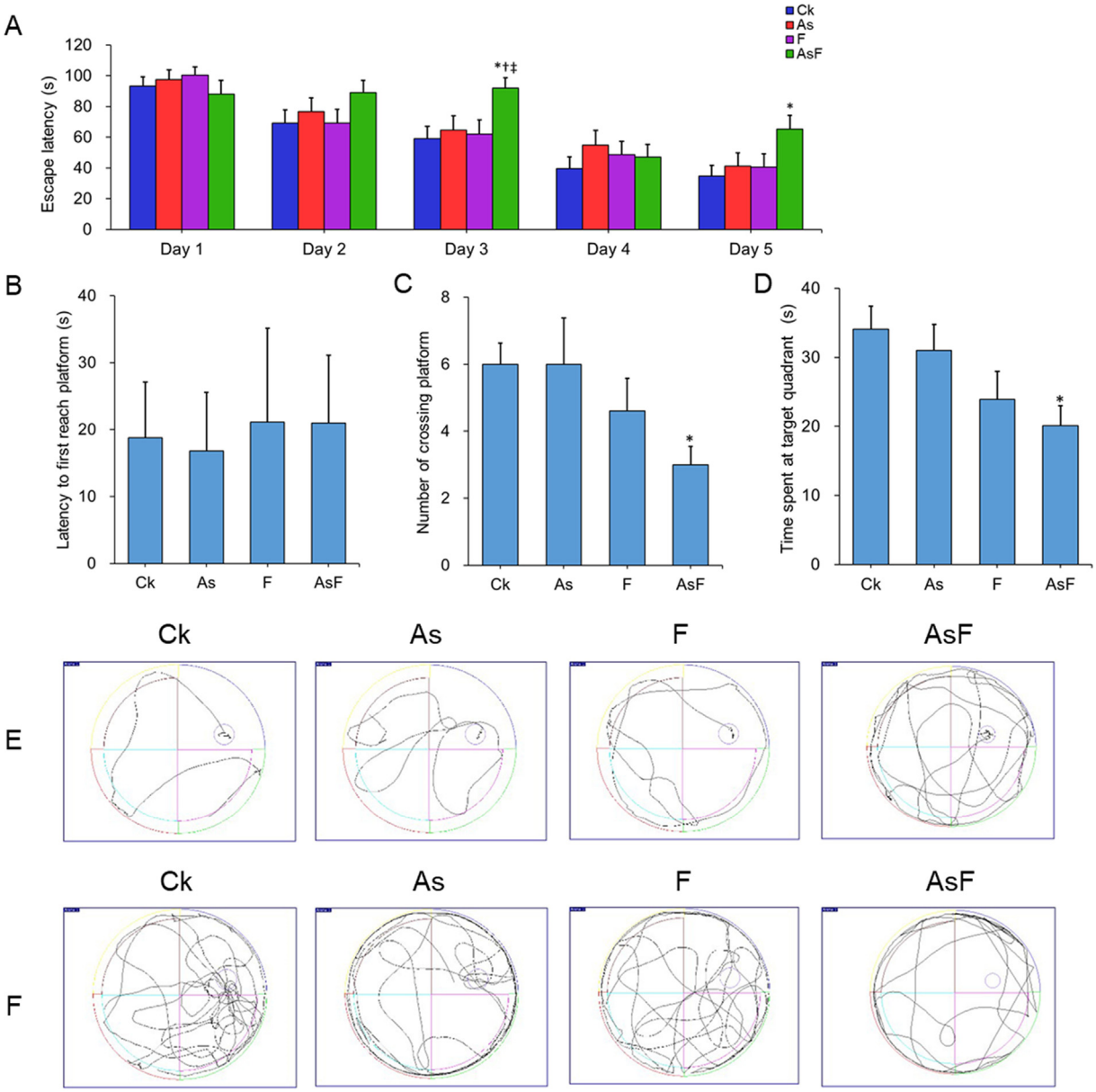

Fig. 1. Effects of iAs, F^- or their combination on spatial learning and memory of rats in Morris water maze test. (A) Escape latency in space navigation training. (B) Latency to first reach platform, (C) Number of times crossing platform and (D) Time spent at target quadrant in space exploration task. (E) Representative swim trajectories of each group at the fifth day of space navigation training. (F) Representative swim trajectories of each group in space exploration task. The data are presented as mean ± SEM (n = 5); *$P < 0.05$ vs. control group, $^{\dagger}P < 0.05$ vs. As group, $^{\ddagger}P < 0.05$ vs. F group.

addition, rats treated with combined AsF were significantly slower than other groups in locating the platform.

In the following space exploration task without platform, the performance of rats was assessed at three aspects within the 120-second time frame: the latency to first reach the former platform position, number of times crossing platform position, and the residence time spent at target quadrant where the hidden platform had been previously placed. Although rats in the F^- alone and AsF combination groups took a relatively longer amount of time to reach the platform position, no statistical significance was detected among groups (Fig. 1B). As shown in Fig. 1C and D, the results indicated that the number of times crossing the platform and time spent at target quadrant of rats in the AsF combination group significantly decreased, as compared with the control group. Despite spending relatively less time at the target quadrant, the iAs or F^- alone group showed no statistically significant difference in contrast to the control group. According to representative trajectories (Fig. 1F) taken by rats during the space exploration task, compared with the control group, rats from exposure groups spent more time swimming against the inner wall of the pool; furthermore, rats in the AsF combination group were the least target-orientated and moved along the wall the most frequently.

3.2. *Effects of iAs and F^-, alone or in combination, on long-term potentiation (LTP) of hippocampus CA1 region*

The results in Fig. 2A illustrate the changes of fEPSP at hippocampal LTP induced by HFS. The fEPSP of all groups decreased downward along with time in the 60-minute recording window. At each representative time point (1 min, 30 min, 60 min), the normalized fEPSP amplitude of iAs and/or F^- exposure groups were consistently lower

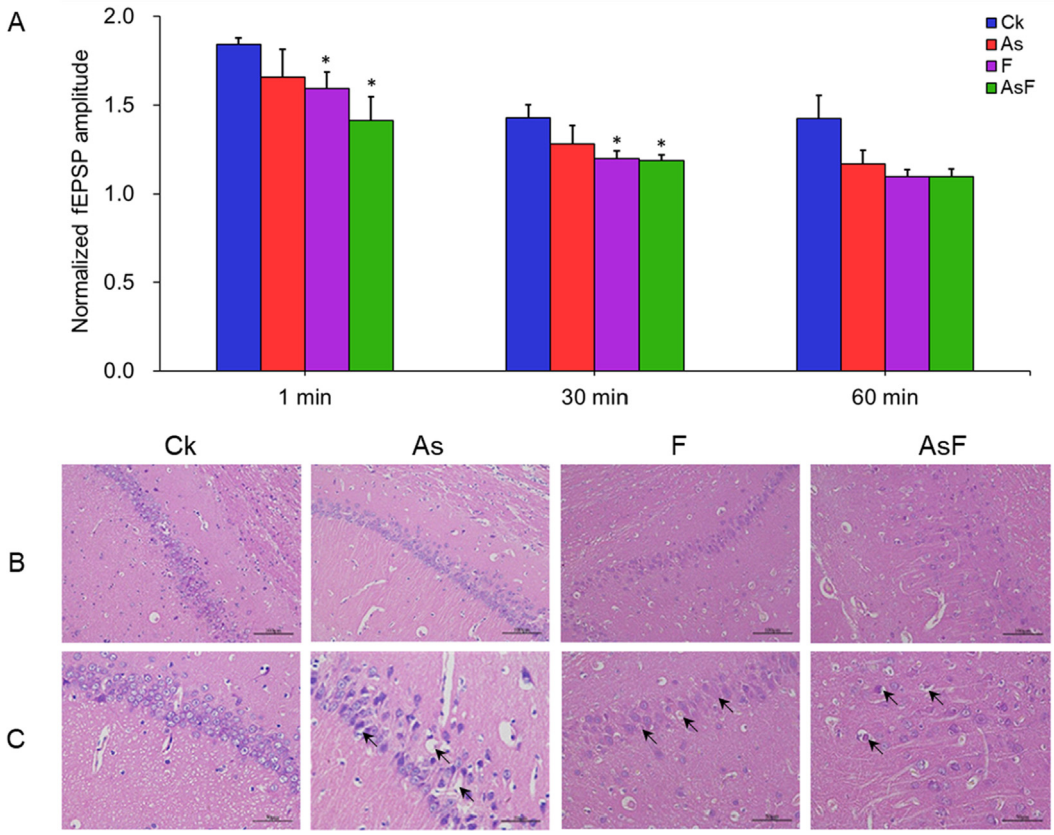

Fig. 2. Effects of iAs, F^- or their combination on LTP and pathological changes in hippocampal CA1 region. (A) Changes of field excitatory postsynaptic potential (fEPSP) at hippocampal CA1 LTP induced by high-frequency stimulation. (B) Representative images of hippocampal neurons stained with H&E (Bar = 100 μm). (C) Representative images of hippocampal neurons stained with H&E (Bar = 50 μm). Arrow marks indicate neural cells with pathological changes. The data are presented as mean ± SEM (n = 5); *$P < 0.05$ vs. control group.

Table 1
Richness and diversity indices of bacterial communities for control and iAs and/or F^- exposure groups.

Group	No. of reads	No. of OTUs	ACE	Chao1	Shannon
Ck	40,173	456	152.79 ± 20.84	152.80 ± 20.81	6.02 ± 0.31
As	43,208	578	189.52 ± 32.10	190.40 ± 32.46	6.04 ± 0.70
F	51,876	542	192.75 ± 7.59	193.32 ± 7.34	6.25 ± 0.14
AsF	45,691	486	184.37 ± 20.36	184.84 ± 20.60	6.24 ± 0.38

than the control group. In particular, as compared with the control group, the fEPSP of F^- alone and AsF combination group demonstrated significant differences at the 1-minute and 30-minute recording points. Surprisingly, no statistically significant differences were detected among groups at the 60-minute time point.

3.3. Effects of iAs and F^-, alone or in combination, on pathological changes in the hippocampal CA1 region

H&E staining of neuron in the hippocampal CA1 region was observed at different optical microscope magnifications (Bar = 100 μm and 50 μm in Fig. 2B & C respectively). In the control group, hippocampal CA1neurons were tightly organized and had multiple cell layers, with healthy cell morphology and clearly stained nuclei and nucleoli. Compared with the control group, hippocampal CA1 neuron pathological changes were observed in iAs and/or F^- exposure groups, including neurofibrillary degeneration, loosely and irregularly organized structure, fewer cell layers, cytoplasmic cavitation, deeper staining of cytoplasm and nuclear pyknosis. In the iAs exposure group, the cytoplasm of the neuronal cells deepened markedly, and the neuronal fibers were swollen. In the F^- exposure group, neuronal cells were loosely and disorderly organized, and some swollen neuronal fibers were observed. In the AsF combination group, the structure of neuronal cells was even looser and more irregular. The number of cell layers and cell quantities significantly decreased, along with increased swollen neuronal fibers and cells with cytoplasmic cavitation.

3.4. Overall structure of bacterial communities across samples

In this study, 20 samples from 4 exposure groups were sequenced using the Illumina MiSeq system. Based on quality-filtering results, one of the samples in the iAs group was excluded as an outlier. As shown in Table 1, after quality trimming and chimera checking, a total of 180,948 high-quality sequences were identified for downstream analysis, with an average of 9,524 reads per sample. After taxonomic assignment, 1,105 operational taxonomic units (OTUs) were obtained. In particular, 456 species-level OTUs in the control group, 578 OTUs in the iAs exposure group, 542 OTUs in the F^- exposure group and 486 OTUs in the AsF combination group were obtained. A variety of indices were employed to estimate the alpha-diversity of the bacterial community based on OTU levels. Among them, the ACE and Chao1 were used to estimate microbial richness, while Shannon was used to evaluate microbial diversity. The results of ACE and Chao1 showed that the iAs and/or F^- exposure groups had a higher bacterial abundance than the control group, although the difference was not significant ($P > 0.05$). Similarly, the higher Shannon index indicated relatively greater bacterial diversity of groups in response to iAs and/or F^- exposure.

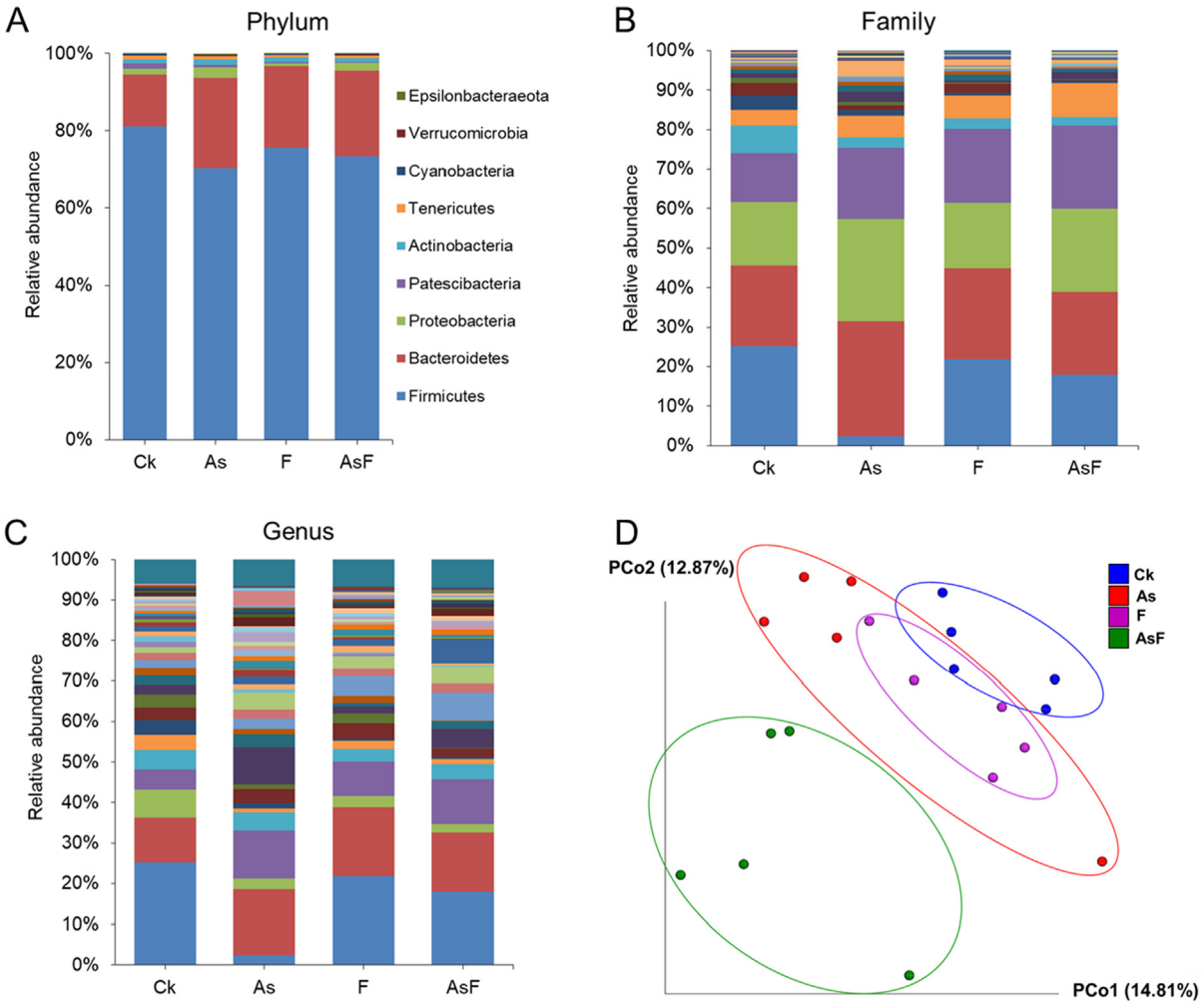

Fig. 3. Overall structure of bacterial communities across samples in response to iAs and/or F⁻ exposure. (A) Bacterial community compositions at phylum level. (B) Bacterial community compositions at family level (legend of taxonomic assignments is provided in Fig. S2 in Supplementary Material). (C) Bacterial community compositions at genus level (legend of taxonomic assignments is provided in Fig. S4 in Supplementary Material). (D) The microbiome patterns of control and exposure groups differentiated by unsupervised principal coordinates analysis (PCoA) of Bray-Curtis dissimilarity.

3.5. Altered microbiome changes in response to iAs and/or F⁻ exposure

The 16S rRNA sequences were assigned from phylum to species levels. As shown in Fig. 3A, at the phylum level, 9 bacterial phyla were identified in each control and exposure group. Firmicutes (70.3%-81.1%) and Bacteroidetes (13.4%–23.3%) were predominant phyla in the gut bacterial community of rats, followed by Proteobacteria (0.8%-2.7%), Patescibacteria (0.2%-1.3%), Actinobacteria (1.0%-1.2%), Tenericutes (0.6%-1.0%) and three phyla with relative abundance < 0.5%, Cyanobacteria, Verrucomicrobia and Epsilonbacteraeota. The exposure groups and control group showed statistically significant differences with regard to Firmicutes, Bacteroidetes, Patescibacteria and Epsilonbacteraeota (Fig. S1 in Supplementary Material). Compared with the control group, exposure to iAs caused significantly lower levels of Firmicutes and higher levels of Bacteroidetes and Epsilonbacteraeota, whereas the relative proportion of Patescibacteria remarkably decreased in response to AsF treatment.

Alterations of gut bacterial composition were also observed at the family level (Fig. 3B). The legend of taxonomic assignments is provided in Fig. S2 in Supplementary Material. There were 11 statistically significant differences between treatment groups and the control group at the family level (Fig. S3 in Supplementary Material). In contrast to the control group, significantly higher relative abundances of Barnesiellaceae, Desulfovibrionaceae, Helicobacteraceae and Prevotellaceae were found in the iAs group; similar differences were also observed at Peptococcaceae and Rikenellaceae in the F⁻ group, and Muribaculaceae in the AsF combination group. Clostridiaceae 1 and Saccharimonadaceae in the AsF group, as well as Lactobacillaceae in the iAs group were notably less abundant than those in the control group. It is worth noting that Peptostreptococcaceae decreased significantly in all three exposure groups.

The microbiome compositions of different groups were also compared at the genus level (Fig. 3C). The legend of taxonomic assignments at the genus level is shown in Fig. S4 in Supplementary Material. The relative abundances of 31 genera differed remarkably between exposure groups and the control group (Table S1 in Supplementary Material), including 11 predominant and 20 less-predominant (< 1% of the total sequences in all groups) genera.

The overall difference in the gut microbiome community structure resulting from iAs and/or F⁻ exposure was evaluated using unsupervised PCoA of Bray-Curtis dissimilarity (Fig. 3D). Principal coordinates 1 and 2 (PCo1 and PCo2) explained 14.81% and 12.87% of the variation in Bray-Curtis dissimilarity, respectively. The clusters of exposure groups were differentiated from control group to different extents. However, the clustering of the iAs or F⁻ group was not separated completely from the control group. Interestingly, the AsF combination group samples were clustered separately from the other three groups.

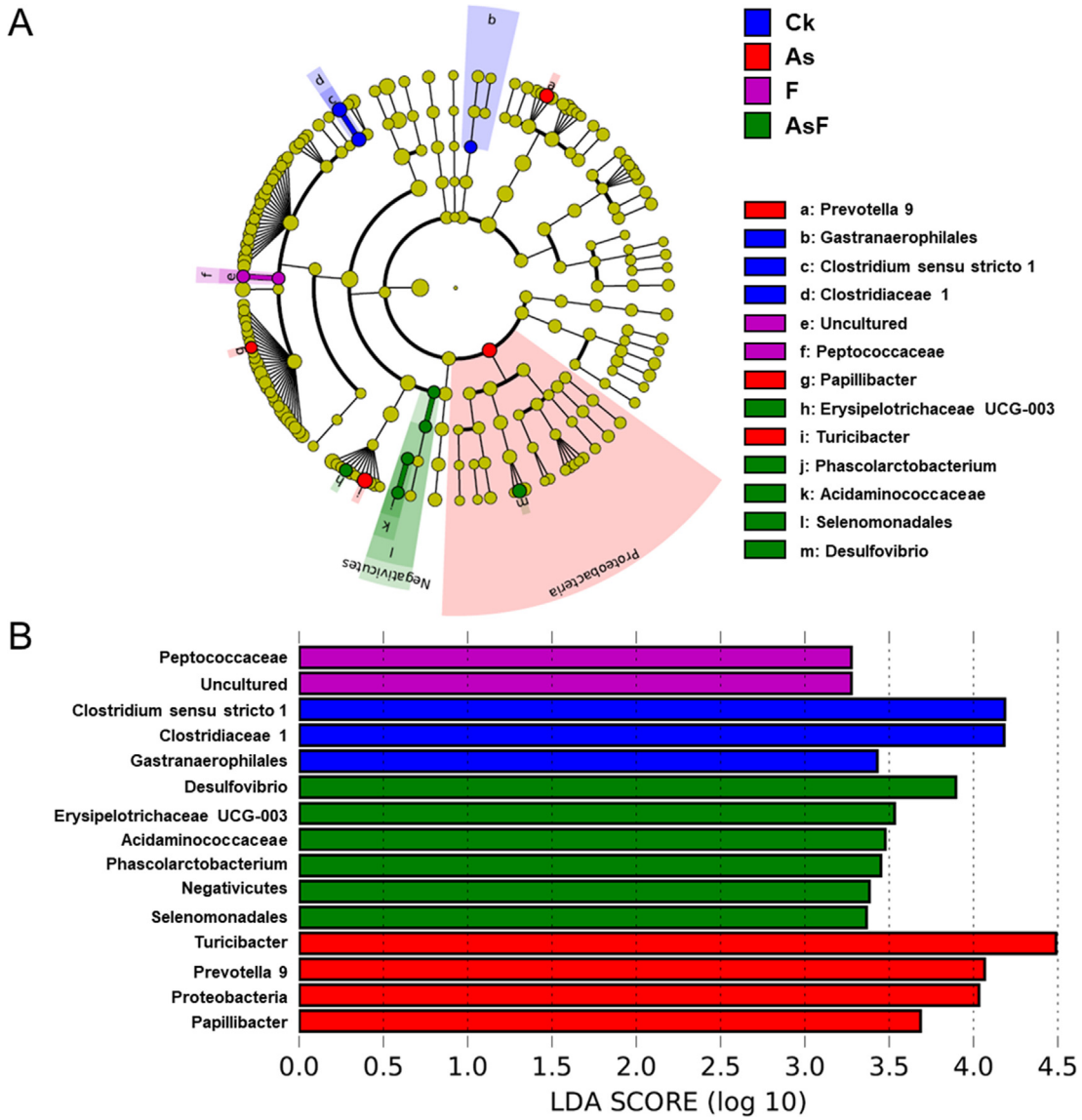

Fig. 4. Distinct taxa identified among groups by linear discriminant analysis effect size (LEfSe) analysis. (A) Cladogram constructed based on the LEfSe analysis to indicate the phylogenetic distribution of taxa that were significantly enriched among groups. The size of each dot is proportional to its effect size. (B) Taxa meeting a linear discriminant analysis (LDA) score significant threshold > 2.

3.6. LEfSe analysis to identify characterization of microorganismal features

A taxonomic cladogram representing the gut microbiome community structure and its predominantly characteristic taxa is shown in Fig. 4A. Only the taxa meeting a linear discriminant analysis (LDA) significant threshold > 2 are displayed (Fig. 4B). These taxa were significantly more abundance in comparison to the other groups. Based on the plots, the order of Gastranaerophilales, family of Clostridiaceae 1 and genus of *Clostridium sensu stricto 1* were enriched in the control group; the phylum of Proteobacteria and three genera, namely *Papillibacter*, *Prevotella 9* and *Turicibacter*, were more abundant in the iAs exposure group; the family of Peptococcaceae and its uncultured genus were enriched in F^- exposure group; the class of Negativicutes, order of Selenomonadales, family of Acidaminococcaceae, as well as three genera *Erysipelotrichaceae UCG-003*, *Desulfovibrio* and *Phascolarctobacterium* were more dominant in samples in response to the AsF combination exposure. The greatest number of featured taxa identified in the AsF group was consistent with its farthest variation distance observed in the previous PCoA result (Fig. 3D).

3.7. Correlations between microbiome composition and water maze performance of rats

In order to investigate the functional correlations between microbiome composition and neurodevelopmental behaviors, the correlation matrix was generated using Pearson's correlation coefficient based on the bacterial genus level, which provides more specific information concerning taxonomic assignments. Here, we focused on the genera with significant difference between the iAs and/or F^- exposure groups and the control group. As shown in the heat map (Fig. 5), clear moderate correlations ($0.5 \leq |r| < 0.7$, $P < 0.05$, highlighted as black-outline squares) and strong correlations ($|r| \geq 0.7$, $P < 0.05$, highlighted as green-outline squares) were identified between significant genera and the three performance indicators (latency to first reaching the platform, number of times crossing the platform, time spent at the target quadrant) of rats in the water maze test.

The correlation matrix shown in Fig. 5A was established by pooling samples from all groups. We identified ten genera that significantly correlated with the three performance indicators of the water maze test. Although no significant difference was observed at latency to first

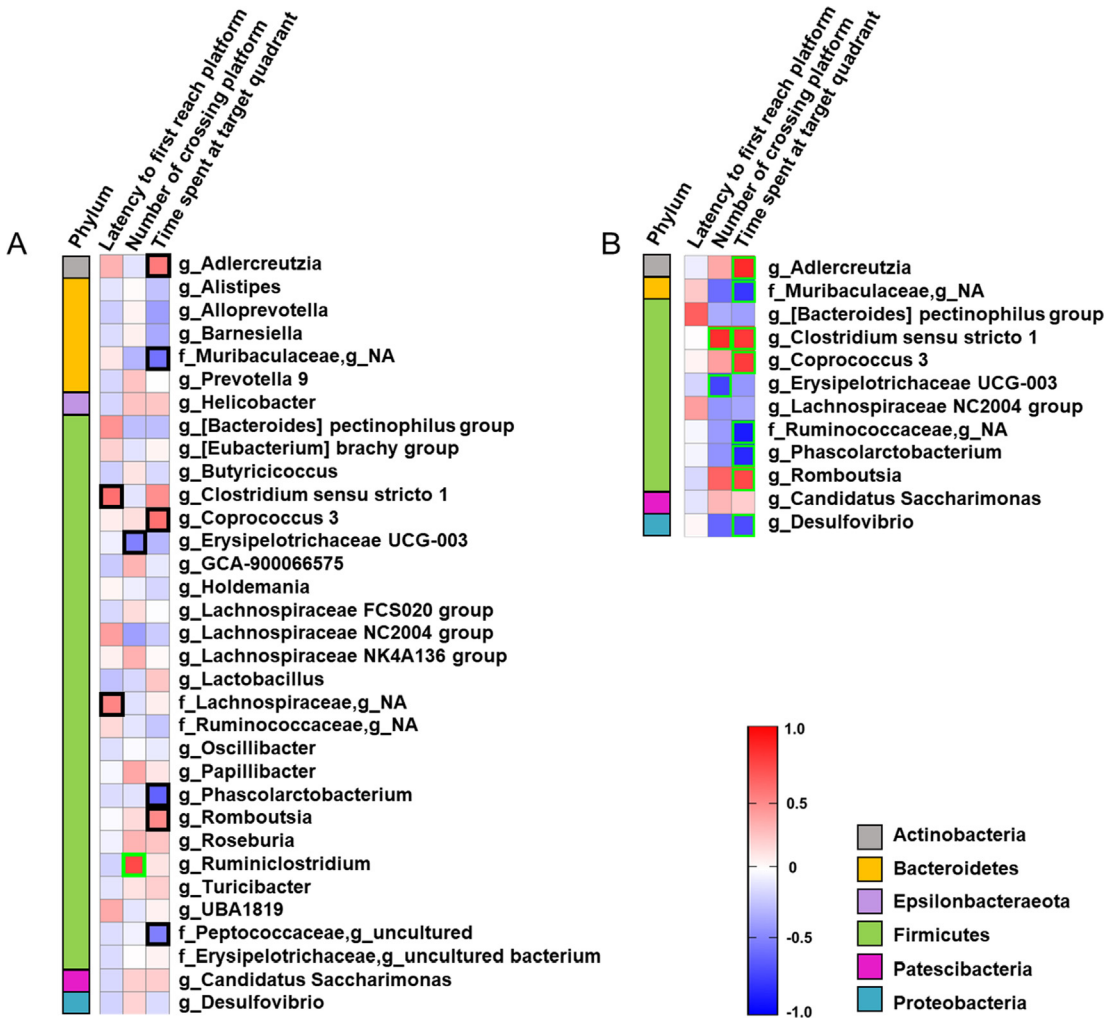

Fig. 5. Correlations between microbiome composition at genus level and neurodevelopmental behaviors of rats in water maze test. (A) Heat map of correlation matrix generated based on all groups. (B) Heat map of correlation matrix generated based on control group and AsF combination exposure group. Moderate correlations ($0.5 \leq |r| < 0.7$, $P < 0.05$) are highlighted as black-outline squares; strong correlations ($|r| \geq 0.7$, $P < 0.05$) are highlighted as green-outline squares.

reaching the platform among these groups, *Clostridium sensu stricto 1* and an unclassified genus in family Lachnospiraceae positively correlated with this variable. In terms of residence time spent at the target quadrant, *Adlercreutzia*, *Coprococcus 3* and *Romboutsia* showed positive correlations with this variable; while *Phascolarctobacterium*, an unclassified genera in family Muribaculaceae and an uncultured bacterium in family Peptococcaceae demonstrated negative correlations. Among these genera, *Ruminiclostridium* was the only taxon demonstrating significantly strong correlation ($r = 0.72$).

Because the AsF combination exposure group was more distinctly differentiated from the control group according to the PCoA analysis, it is worth exploring the correlations between neurodevelopmental behaviors of rats and the genera that showed significant changes specifically between the AsF and control groups. As shown in Fig. 5B, 9 out of 12 genera showed significant correlations with two of the water maze performance indicators; number of times crossing the platform and time spent at the target quadrant. Intriguingly, all correlations were strong ($r = 0.70$–0.90). More explicitly, *Clostridium sensu stricto 1* was positively correlated with number of times crossing the platform, while *Erysipelotrichaceae UCG-003* had an inverse correlation with this indicator. The variable, time spent at the target quadrant, showed significant positive correlation with four genera, which were *Adlercreutzia*, *Clostridium sensu stricto 1*, *Coprococcus 3*, *Romboutsia*, and were inversely correlated with *Phascolarctobacterium*, *Desulfovibrio* and two unclassified genera in family Muribaculaceae and Ruminococcaceae.

4. Discussion

Toxicity induced by iAs and F^- has attracted great interest in scientific and medical societies due to their threats to public health worldwide. Numerous studies have suggested that iAs and F^- alone or concurrent exposure could produce adverse effects on neurobehavioral and cognitive functions of children and rodent models when exposure occurs during early life, and the joint actions of iAs and F^- could potentially pose a greater risk (Wang et al., 2007; Jiang et al., 2014; Tsai et al., 2003; Vibol et al., 2015; Rodriguez-Barranco et al., 2013; Borman and Fyfe, 2013; Das, 2016; Sebastian and Sunitha, 2015; Bashash et al., 2017; Grandjean and Landrigan, 2014). Increasing evidences show that iAs or F^- exposure has a remarkable impact on the gut and/or oral microbiome (Chi et al., 2016; Dheer et al., 2015; Isokpehi et al., 2014; Koopman et al., 2015; Lu et al., 2014; Chen et al., 2013; Reilly et al., 2016; Bisanz et al., 2014; Ghaisas et al., 2016; Yasuda et al., 2017; Luo et al., 2016), some of which have been linked to neurodevelopment and behavior. In this study, we first time provide data showing that concurrent iAs and F^- exposure led to more prominent effects on neurodevelopment and gut microbiome composition structures in rats, and some bacterial genera are strongly correlated ($r = 0.70$–0.90) with observed differences in spatial learning and memory performance

between the control and concurrent exposure groups.

The Morris water maze test is a widely used method for assessing the spatial learning and memory ability of rodents, which in turn reflects central nervous system function in animals. In our present study, in comparison with the control group, the rats that were exposed to iAs and F^-, alone or in combination, exhibited a significant delay in finding the hidden platform on the third and fifth day of space navigation training, while the iAs and F^- mixture group was the most significant one. Furthermore, iAs and F^- mixture group also showed a significant decrease of the number of times crossing platform and time spent at target quadrant. LTP of synaptic transmission in the hippocampus is the major form of activity-dependent plasticity in the central nervous system and serves as a key synaptic model for investigating the cellular and molecular mechanisms of spatial learning and memory (Bliss and Collingridge, 1993). Similarly, the changes of the LTP and the fEPSP were more notable in the iAs and F^- combination exposure group. These results suggest that exposure to iAs and F^- may impair both spatial learning and memory performance in rats, and the influences induced by concurrent exposure is more prominent than iAs or F^- alone. The findings were largely consistent with the results of previous animal experimental studies and epidemiological investigations (Wang et al., 2007; Jiang et al., 2014; Wu et al., 2006; Zhang et al., 1999). The hippocampus is essential for memory acquisition, storage, recall and reconstruction (Jarrard, 1993). Some studies indicate that arsenic induces hippocampal-dependent behavioral deficits in rodent models, which may lead to impairment of spatial memory (Liu et al., 2012; Krüger et al., 2006). Our H&E staining results showed that hippocampal neuron pathological changes were observed in all exposure groups, which provide further evidence and support the association.

Numerous studies report that a shift in gut microbiome composition profiles has been implicated as a pathologic indictor in various diseases (Thursby and Juge, 2017; Round and Mazmanian, 2009; Marchesi et al., 2016). In this study, we identified a number of significant changes at different taxonomic levels (phylum, family, and genus) of microbial communities in response to iAs and/or F^- exposure. Through PCoA analysis based on OTU level, the subjects treated with combined iAs and F^- were distinctly separated from the other three groups; further LEfSe analysis indicated the predominantly characteristic taxa, with the greatest number of featured taxa identified in the AsF combination group. These results suggested concurrent iAs and F^- exposure had a more prominent impact on gut microbial composition structures in rats.

Increasing evidence has suggested the perturbations of microbial communities could result in developmental deficits in neurobehavioral and cognitive functions (Borre et al., 2014; Galland, 2014; Scheperjans et al., 2015; Mulle et al., 2013; De Angelis et al., 2013). Alteration of gut microbiota profiles has been suggested to influence neurological functions and behaviors potentially through immune activation, amino acid metabolism, neurotransmitters, and neuroactive bacterial metabolites such as short-chain fatty acid, *via* the mechanisms of communication along the microbiota–gut–brain axis (Cryan and Dinan, 2012; Mohajeri et al., 2018). Dysregulation of the microbiota–gut–brain axis may contribute to the development of psychiatric diseases (Fond et al., 2014). A research has linked the influence of the gut microbiota on neurological behavior with changes in the hippocampus. Remarkable alteration in the dendritic morphology of the hippocampus was observed between germ-free mice and conventionally colonized mice, suggesting the crucial role of gut microbiota in maintaining normal morphology and ultrastructure of brain neurons (Luczynski et al., 2016). The finding, at least, partially support the contribution of perturbed gut microbiota profiles to pathological changes of hippocampal neuron observed in our study. In current study, a correlation analysis between indices of the water maze test and microbial composition at the genus level identified featured genera that were clearly associated with neurobehavioral performance of rats. 75% (9 out of 12) genera, which had a remarkable difference in relative abundance between the control and AsF combination groups, showed significantly strong correlations (r = 0.70–0.90) with two of the water maze performance indicators. Specifically, *Adlercreutzia*, *Clostridium sensu stricto 1*, *Coprococcus 3* and *Romboutsia* showed strong positive correlations with task performance. Recent studies have reported that a decreased abundance of *Adlercreutzia* is associated with multiple sclerosis in patients through affecting brain inflammatory signaling, implying its regulating effect on immune response in central neural system (Chen et al., 2016; Camara-Lemarroy et al., 2018). A more recent study found a negative correlation between *Adlercreutzia* abundance and anxiety-like behaviors, suggesting an association with neuropsychic behaviors (Xu et al., 2019). In addition, *Adlercreutzia* pertain to the phylum of Actinobacteria, which was reported to act a pivotal part in depressive-like behaviors through perturbing host's amino acid metabolism (Zheng et al., 2016). *Clostridium sensu stricto 1* belongs to the family of Clostridiaceae, which was reported to be less abundant in patients with Alzheimer's disease (Vogt et al., 2017). *Coprococcus* is known to produce the short-chain fatty acid butyrate, which strengthens the epithelial defense barrier and reduces intestinal inflammation (Louis et al., 2014), and it has been reported to be depleted in patients with major depressive disorder (Levenson et al., 2004). A study demonstrated that butyrate is capable of mediating enhanced induction of long term potentiation at in CA1 region of the hippocampus in rats through the extracellular signal regulated kinase-dependent signaling mechanism (Lattal et al., 2007); which was subsequently confirmed by another study that butyrate facilitates neuronal plasticity and enhances memory formation (Valles-Colomer et al., 2019). Furthermore, a recent study suggested that *Coprococcus* was consistently associated with greater quality of life (Gao et al., 2018). *Romboutsia* is a member of the family Peptostreptococcaceae, which was found to be related to inflammatory bowel disease triggered by chronic stress (Leng et al., 2016), a higher proportion of which was reported in gut microbial communities of healthy animals than in those with dysbiosis of the intestinal microbiota (Kaakoush, 2015). On the other hand, strong inverse correlations were identified between five genera (*Erysipelotrichaceae UCG-003*, *Phascolarctobacterium*, *Desulfovibrio* and two unclassified genera in family Muribaculaceae and Ruminococcaceae) and space exploration task indices. Few studies have reported the relationship between *Erysipelotrichaceae UCG-003* and health outcomes. However, at the corresponding family level, Erysipelotrichaceae is strongly associated with gastrointestinal diseases and metabolic disorders (Chen et al., 2012), suggesting its key role in inflammation-related disorders. Relative abundance of Erysipelotrichaceae was reported to be elevated in colorectal cancer patients as compared to healthy controls (Jiang et al., 2015). Increasing evidence has linked higher abundance of *Phascolarctobacterium* to various neurodevelopmental and inflammation-related diseases, including Alzheimer's disease (Vogt et al., 2017), major depressive disorder (Weir et al., 2013) and colorectal cancer (Walecki et al., 2018). *Desulfovibrio* is one of the main microorganisms producing propionic acid (PPA) and its related short-chain fatty acid, which can cause symptoms similar to autism spectrum disorder (ASD) (MacFabe, 2012). *Desulfovibrio* was also reported to produce hydrogen sulfide, a possible mitochondrial toxin, featuring both neurotoxic and colonotoxic effects synergistic to PPA (Petra et al., 2015). Studies have shown *Desulfovibrio* is over-represented in children with ASD (Li et al., 2017; Finegold, 2011; Chou, 2019). Although two of the featured genera had no classification information, implication regarding health conditions could still be attained from their upper family level. Muribaculaceae was recently reported to be more abundant in patients with Parkinson's disease than healthy controls (Williams et al., 2011). Cumulative levels of Ruminococcaceae were found in children patients with ASD-gastrointestinal symptoms [95] and cohorts with major depressive disorder (Levenson et al., 2004); indicating its role in neurodevelopmental dysbiosis. Although accumulated evidence provides supporting for the associations between featured bacterial genera and neurological behaviors observed in our current study, further studies (e.g. targeted bacterial species transplantation, functional assessment of gut microbiome, changes of

related biomarkers at lesion locations) are warranted to validate the casual effects of featured bacterial genera and elucidate the mechanisms underpinning the ability of altered microbiota profiles to affect host's neurological behaviors.

5. Conclusion

In summary, our present study evaluated neurotoxicity and gut microbiome disturbance as a result of exposure to high-dose of iAs and F^-, alone or in combination, from early life (*in utero* and childhood) to puberty in rats. iAs and/or F^- exposure led to neurobehavioral deficits in spatial learning and memory, most prominently in offspring rats co-exposed to iAs and F^-. The H&E staining results confirmed that iAs and/or F^- caused pathological changes in hippocampal neuron. 16S rRNA gene sequencing results demonstrated perturbation of gut microbiome communities at different taxonomic levels in response to iAs and/or F^- exposure. Again, the effects were more noticeable in the AsF combination group. Furthermore, nine genera, which had significant difference of relative abundance between the control and AsF combination groups, were identified to have significantly strong correlation (r = 0.70–0.90) with spatial learning and memory performance. Collectively, these results suggest that concurrent iAs and F^- exposure led to more prominent effects on neurodevelopment and gut microbiome composition structures in rats, and the strong correlation between them indicates a high potential for the development of novel microbiome-based biomarkers of iAs and/or F^- associated neurodevelopmental deficits.

CRediT authorship contribution statement

Yulan Qiu: Conceptualization, Methodology, Validation, Resources, Writing - review & editing, Project administration, Funding acquisition. **Xushen Chen:** Formal analysis, Writing - original draft, Visualization. **Xiaoyan Yan:** Conceptualization, Methodology, Funding acquisition. **Jie Wang:** Methodology, Software, Data curation. **Guan Yu:** Methodology, Software, Data curation. **Wenyan Ma:** Investigation, Formal analysis, Visualization. **Bo Xiao:** Formal analysis, Visualization. **Sarah Quinones:** Formal analysis, Visualization. **Xiaolin Tian:** Investigation, Visualization. **Xuefeng Ren:** Conceptualization, Methodology, Writing - review & editing, Supervision, Funding acquisition.

Declaration of Competing Interest

The authors declared that there is no conflict of interest.

Acknowledgement

This study was supported by National Institutes of Health (NIH) grant ES022629 (to X.R.). Additionally, it was supported by National Natural Science Foundation of China (No. 81773405 to Y.Q.) and the Postdoctoral Science Foundation of China (2016M600199 to X.Y.) and the Program for the Outstanding Innovative Teams of Higher Learning Institute of Shanxi (to X.Y.).

Appendix A. Supplementary material

Supplementary data to this article can be found online at https://doi.org/10.1016/j.envint.2020.105763.

References

Alarcon-Herrera, M.T., Bundschuh, J., Nath, B., Nicolli, H.B., Gutierrez, M., Reyes-Gomez, V.M., Nunez, D., Martin-Dominguez, I.R., Sracek, O., 2013. Co-occurrence of arsenic and fluoride in groundwater of semi-arid regions in Latin America: genesis, mobility and remediation. J. Hazard. Mater. 262, 960–969.

Amini, M., Abbaspour, K.C., Berg, M., Winkel, L., Hug, S.J., Hoehn, E., Yang, H., Johnson, C.A., 2008. Statistical modeling of global geogenic arsenic contamination in groundwater. Environ. Sci. Technol. 42, 3669–3675.

Arshad, N., Imran, S., 2016. Assessment of arsenic, fluoride, bacteria, and other contaminants in drinking water sources for rural communities of Kasur and other districts in Punjab, Pakistan. Environ. Sci. Pollut. Res. Int..

Bancroft, J.D., Gamble, M., 2008. Theory and practice of histological techniques. Elsevier Health Sci.

Bashash, M., Thomas, D., Hu, H., Martinez-Mier, E.A., Sanchez, B.N., Basu, N., Peterson, K.E., Ettinger, A.S., Wright, R., Zhang, Z., et al., 2017. Prenatal Fluoride Exposure and Cognitive Outcomes in Children at 4 and 6–12 Years of Age in Mexico. Environ. Health Perspect. 125, 097017.

Bisanz, J.E., Enos, M.K., Mwanga, J.R., Changalucha, J., Burton, J.P., Gloor, G.B., Reid, G., 2014. Randomized open-label pilot study of the influence of probiotics and the gut microbiome on toxic metal levels in Tanzanian pregnant women and school children. MBio 5, e01580–01514.

Bliss, T.V., Collingridge, G.L., 1993. A synaptic model of memory: long-term potentiation in the hippocampus. Nature 361, 31.

Bolyen, E., Rideout, J.R., Dillon, M.R., Bokulich, N.A., Abnet, C.C., Al-Ghalith, G.A., Alexander, H., Alm, E.J., Arumugam, M., Asnicar, F., et al., 2019. Reproducible, interactive, scalable and extensible microbiome data science using QIIME 2. Nat. Biotechnol. 37, 852–857.

Borman, B., Fyfe, C., 2013. Fluoride and children's IQ. N. Z. Med. J. 126, 111–112.

Borre, Y.E., Moloney, R.D., Clarke, G., Dinan, T.G., Cryan, J.F., 2014. The impact of microbiota on brain and behavior: mechanisms & therapeutic potential. Adv. Exp. Med. Biol. 817, 373–403.

Bretzler, A., Lalanne, F., Nikiema, J., Podgorski, J., Pfenninger, N., Berg, M., Schirmer, M., 2017. Groundwater arsenic contamination in Burkina Faso: Predicting and verifying regions at risk, West Africa. Sci. Total Environ.

Brouwer, I.D., Dirks, O.B., De Bruin, A., Hautvast, J.G., 1988. Unsuitability of World Health Organisation guidelines for fluoride concentrations in drinking water in Senegal. Lancet 1, 223–225.

Buchhamer, E.E., Blanes, P.S., Osicka, R.M., Gimenez, M.C., 2012. Environmental risk assessment of arsenic and fluoride in the Chaco Province, Argentina: research advances. J. Toxicol. Environ. Health A 75, 1437–1450.

Callahan, B.J., McMurdie, P.J., Rosen, M.J., Han, A.W., Johnson, A.J.A., Holmes, S.P., 2016. DADA2: high-resolution sample inference from Illumina amplicon data. Nat. Methods 13, 581.

Camara-Lemarroy, C.R., Metz, L., Meddings, J.B., Sharkey, K.A., Wee Yong, V., 2018. The intestinal barrier in multiple sclerosis: implications for pathophysiology and therapeutics. Brain 141, 1900–1916.

Chakraborti, D., Das, B., Murrill, M.T., 2011. Examining India's groundwater quality management. Environ. Sci. Technol. 45, 27–33.

Chen, B., Cao, F., Yuan, C., Lu, X., Shen, S., Zhou, J., Le, X.C., 2013. Arsenic speciation in saliva of acute promyelocytic leukemia patients undergoing arsenic trioxide treatment. Anal. Bioanal. Chem. 405, 1903–1911.

Chen, J., Chia, N., Kalari, K.R., Yao, J.Z., Novotna, M., Soldan, M.M.P., Luckey, D.H., Marietta, E.V., Jeraldo, P.R., Chen, X., 2016. Multiple sclerosis patients have a distinct gut microbiota compared to healthy controls. Sci. Rep. 6, 28484.

Chen, W., Liu, F., Ling, Z., Tong, X., Xiang, C., 2012. Human intestinal lumen and mucosa-associated microbiota in patients with colorectal cancer. PLoS ONE 7, e39743.

Chi, L., Bian, X., Gao, B., Ru, H., Tu, P., Lu, K., 2016. Sex-Specific Effects of Arsenic Exposure on the Trajectory and Function of the Gut Microbiome. Chem. Res. Toxicol. 29, 949–951.

Chioca, L.R., Raupp, I.M., Da Cunha, C., Losso, E.M., Andreatini, R., 2008. Subchronic fluoride intake induces impairment in habituation and active avoidance tasks in rats. Eur. J. Pharmacol. 579, 196–201.

Choi, A.L., Sun, G., Zhang, Y., Grandjean, P., 2012. Developmental fluoride neurotoxicity: a systematic review and meta-analysis. Environ. Health Perspect. 120, 1362–1368.

Chou, H.-C., 2019. The Association of Gut Microbiome Composition and Parkinson's Disease in Patient Cohort of. Central California. UCLA.

Council, N.R., 2006. Fluoride in Drinking Water: A Scientific Review of EPA's Standards. The National Academies Press, Washington, DC.

Cryan, J.F., Dinan, T.G., 2012. Mind-altering microorganisms: the impact of the gut microbiota on brain and behaviour. Nat. Rev. Neurosci. 13, 701–712.

Das, K., 2016. Mondal NK: Dental fluorosis and urinary fluoride concentration as a reflection of fluoride exposure and its impact on IQ level and BMI of children of Laxmisagar, Simlapal Block of Bankura District, W.B., India. Environ. Monit. Assess. 188, 218.

De Angelis, M., Piccolo, M., Vannini, L., Siragusa, S., De Giacomo, A., Serrazzanetti, D.I., Cristofori, F., Guerzoni, M.E., Gobbetti, M., Francavilla, R., 2013. Fecal microbiota and metabolome of children with autism and pervasive developmental disorder not otherwise specified. PLoS ONE 8, e76993.

Dheer, R., Patterson, J., Dudash, M., Stachler, E.N., Bibby, K.J., Stolz, D.B., Shiva, S., Wang, Z., Hazen, S.L., Barchowsky, A., Stolz, J.F., 2015. Arsenic induces structural and compositional colonic microbiome change and promotes host nitrogen and amino acid metabolism. Toxicol. Appl. Pharmacol. 289, 397–408.

Finegold, S.M., 2011. Desulfovibrio species are potentially important in regressive autism. Med. Hypotheses 77, 270–274.

Fond, G., Loundou, A., Hamdani, N., Boukouaci, W., Dargel, A., Oliveira, J., Roger, M., Tamouza, R., Leboyer, M., Boyer, L., 2014. Anxiety and depression comorbidities in irritable bowel syndrome (IBS): a systematic review and meta-analysis. Eur. Arch. Psychiatry Clin. Neurosci. 264, 651–660.

Galland, L., 2014. The gut microbiome and the brain. J. Med. Food 17, 1261–1272.

Gao, X., Cao, Q., Cheng, Y., Zhao, D., Wang, Z., Yang, H., Wu, Q., You, L., Wang, Y., Lin, Y., 2018. Chronic stress promotes colitis by disturbing the gut microbiota and

triggering immune system response. Proc. Natl. Acad. Sci. 115, E2960–E2969.
Ghaisas, S., Maher, J., Kanthasamy, A., 2016. Gut microbiome in health and disease: Linking the microbiome-gut-brain axis and environmental factors in the pathogenesis of systemic and neurodegenerative diseases. Pharmacol. Ther. 158, 52–62.
Goldhaber, M.B., Hatch, J.R., Pashin, J.C., Offield, T.W., Finkelman, R.B., 1997. Anomalous arsenic and fluorine concentrations in carboniferous coal, Black Warrior Basin, Alabama: Evidence for fluid expulsion during Alleghanian thrusting. Geological Society of America Annual Meeting Abstracts with Programs, Boulder, Colorado: GSA 51.
Gonzalez-Horta, C., Ballinas-Casarrubias, L., Sanchez-Ramirez, B., Ishida, M.C., Barrera-Hernandez, A., Gutierrez-Torres, D., Zacarias, O.L., Saunders, R.J., Drobna, Z., Mendez, M.A., et al., 2015. A concurrent exposure to arsenic and fluoride from drinking water in Chihuahua, Mexico. Int. J. Environ. Res. Public Health 12, 4587–4601.
Grandjean, P., Landrigan, P.J., 2014. Neurobehavioural effects of developmental toxicity. Lancet Neurol. 13, 330–338.
Hoen, A.G., Madan, J.C., Li, Z., Coker, M., Lundgren, S.N., Morrison, H.G., Palys, T., Jackson, B.P., Sogin, M.L., Cottingham, K.L., Karagas, M.R., 2018. Sex-specific associations of infants' gut microbiome with arsenic exposure in a US population. Sci. Rep. 8, 12627.
Humans IWGotEoCRt, Some drinking-water disinfectants and contaminants, including arsenic IARC Monogr Eval Carcinog Risks Hum 84 2004 1 477.
Isokpehi, R.D., Udensi, U.K., Simmons, S.S., Hollman, A.L., Cain, A.E., Olofinsae, S.A., Hassan, O.A., Kashim, Z.A., Enejoh, O.A., Fasesan, D.E., Nashiru, O., 2014. Evaluative profiling of arsenic sensing and regulatory systems in the human microbiome project genomes. Microbiol Insights 7, 25–34.
Jarrard, L.E., 1993. On the role of the hippocampus in learning and memory in the rat. Behav. Neural. Biol. 60, 9–26.
Jiang, H., Ling, Z., Zhang, Y., Mao, H., Ma, Z., Yin, Y., Wang, W., Tang, W., Tan, Z., Shi, J., 2015. Altered fecal microbiota composition in patients with major depressive disorder. Brain Behav. Immun. 48, 186–194.
Jiang, S., Su, J., Yao, S., Zhang, Y., Cao, F., Wang, F., Wang, H., Li, J., Xi, S., 2014. Fluoride and arsenic exposure impairs learning and memory and decreases mGluR5 expression in the hippocampus and cortex in rats. PLoS ONE 9, e96041.
Kaakoush, N.O., 2015. Insights into the role of Erysipelotrichaceae in the human host. Front. Cell. Infect. Microbiol. 5, 84.
Koopman, J.E., van der Kaaij, N.C., Buijs, M.J., Elyassi, Y., van der Veen, M.H., Crielaard, W., Ten Cate, J.M., Zaura, E., 2015. The Effect of Fixed Orthodontic Appliances and Fluoride Mouthwash on the Oral Microbiome of Adolescents - A Randomized Controlled Clinical Trial. PLoS ONE 10, e0137318.
Krüger, K., Binding, N., Straub, H., Mußhoff, U., 2006. Effects of arsenite on long-term potentiation in hippocampal slices from young and adult rats. Toxicol. Lett. 165, 167–173.
Lattal, K.M., Barrett, R.M., Wood, M.A., 2007. Systemic or intrahippocampal delivery of histone deacetylase inhibitors facilitates fear extinction. Behav. Neurosci. 121, 1125.
Leng, Y., Yi, M., Fan, J., Bai, Y., Ge, Q., Yao, G., 2016. Effects of acute intra-abdominal hypertension on multiple intestinal barrier functions in rats. Sci. Rep. 6, 22814.
Levenson, J.M., O'Riordan, K.J., Brown, K.D., Trinh, M.A., Molfese, D.L., Sweatt, J.D., 2004. Regulation of histone acetylation during memory formation in the hippocampus. J. Biol. Chem. 279, 40545–40559.
Levy, D.B., Schramke, J.A., Esposito, J.K., Erickson, T.A., Moore, J.C., 1999. The shallow ground water chemistry of arsenic, fluorine, and major elements: Eastern Owens Lake California. Appl. Geochem. 14, 53–65.
Li, Q., Han, Y., Dy, A.B.C., Hagerman, R.J., 2017. The gut microbiota and autism spectrum disorders. Front. Cell. Neurosci. 11, 120.
Limon-Pacheco, J.H., Jimenez-Cordova, M.I., Cardenas-Gonzalez, M., Retana, I.M.S., Gonsebatt, M.E., Del Razo, L.M., 2018. Potential Co-exposure to Arsenic and Fluoride and Biomonitoring Equivalents for Mexican Children. Ann. Global Health 84, 257–273.
Liu, S., Piao, F., Sun, X., Bai, L., Peng, Y., Zhong, Y., Ma, N., Sun, W., 2012. Arsenic-induced inhibition of hippocampal neurogenesis and its reversibility. Neurotoxicology 33, 1033–1039.
Liu, J., Wang, H-w, Lin, L., Miao, C-y, Zhang, Y., 2019. Zhou B-h: Intestinal barrier damage involved in intestinal microflora changes in fluoride-induced mice. Chemosphere.
Louis, P., Hold, G.L., Flint, H.J., 2014. The gut microbiota, bacterial metabolites and colorectal cancer. Nat. Rev. Microbiol. 12, 661.
Lu, K., Abo, R.P., Schlieper, K.A., Graffam, M.E., Levine, S., Wishnok, J.S., Swenberg, J.A., Tannenbaum, S.R., Fox, J.G., 2014. Arsenic exposure perturbs the gut microbiome and its metabolic profile in mice: an integrated metagenomics and metabolomics analysis. Environ. Health Perspect. 122, 284–291.
Luczynski, P., Whelan, S.O., O'Sullivan, C., Clarke, G., Shanahan, F., Dinan, T.G., Cryan, J.F., 2016. Adult microbiota-deficient mice have distinct dendritic morphological changes: Differential effects in the amygdala and hippocampus. Eur. J. Neurosci. 44, 2654–2666.
Luo, Q., Cui, H., Peng, X., Fang, J., Zuo, Z., Deng, J., Liu, J., Deng, Y., 2016. Dietary High Fluorine Alters Intestinal Microbiota in Broiler Chickens. Biol. Trace Elem. Res. 173, 483–491.
MacFabe, D.F., 2012. Short-chain fatty acid fermentation products of the gut microbiome: implications in autism spectrum disorders. Microbial ecology in health and disease 23, 19260.
Marchesi, J.R., Adams, D.H., Fava, F., Hermes, G.D., Hirschfield, G.M., Hold, G., Quraishi, M.N., Kinross, J., Smidt, H., Tuohy, K.M., 2016. The gut microbiota and host health: a new clinical frontier. Gut 65, 330–339.
Merola, R.B., Kravchenko, J., Rango, T., Vengosh, A., 2014. Arsenic exposure of rural populations from the Rift Valley of Ethiopia as monitored by keratin in toenails. J. Expo Sci. Environ. Epidemiol. 24, 121–126.
Mohajeri, M.H., La Fata, G., Steinert, R.E., Weber, P., 2018. Relationship between the gut microbiome and brain function. Nutr. Rev. 76, 481–496.
Mulle, J.G., Sharp, W.G., Cubells, J.F., 2013. The gut microbiome: a new frontier in autism research. Curr Psychiatry Rep 15, 337.
Obiri, S., Yeboah, P.O., Osae, S., Adu-Kumi, S., 2016. Levels of arsenic, mercury, cadmium, copper, lead, zinc and manganese in serum and whole blood of resident adults from mining and non-mining communities in Ghana. Environ. Sci. Pollut. Res. Int. 23, 16589–16597.
Ogbu, I.S., Okoro, O.I., Ugwuja, E.I., 2012. Well waters fluoride in Enugu, Nigeria. Int. J. Occup. Environ. Med. 3, 96–98.
Petra, A.I., Panagiotidou, S., Hatziagelaki, E., Stewart, J.M., Conti, P., Theoharides, T.C., 2015. Gut-microbiota-brain axis and its effect on neuropsychiatric disorders with suspected immune dysregulation. Clin. Ther. 37, 984–995.
Quast, C., Pruesse, E., Yilmaz, P., Gerken, J., Schweer, T., Yarza, P., Peplies, J., Glöckner, F.O., 2012. The SILVA ribosomal RNA gene database project: improved data processing and web-based tools. Nucleic Acids Res. 41, D590–D596.
Reilly, C., Goettl, M., Steinmetz, M., Nikrad, J., Jones, R.S., 2016. Short-term effects of povidone iodine and sodium fluoride therapy on plaque levels and microbiome diversity. Oral Dis. 22, 155–161.
Rocha-Amador, D., Navarro, M.E., Carrizales, L., Morales, R., Calderon, J., 2007. Decreased intelligence in children and exposure to fluoride and arsenic in drinking water. Cad. Saude Publica 23 (Suppl 4), S579–587.
Rodriguez-Barranco, M., Lacasana, M., Aguilar-Garduno, C., Alguacil, J., Gil, F., Gonzalez-Alzaga, B., Rojas-Garcia, A., 2013. Association of arsenic, cadmium and manganese exposure with neurodevelopment and behavioural disorders in children: a systematic review and meta-analysis. Sci. Total Environ. 454–455, 562–577.
Rosado, J.L., Ronquillo, D., Kordas, K., Rojas, O., Alatorre, J., Lopez, P., Garcia-Vargas, G., Del Carmen, Caamano M, Cebrian, M.E., Stoltzfus, R.J., 2007. Arsenic exposure and cognitive performance in Mexican schoolchildren. Environ. Health Perspect. 115, 1371–1375.
Round, J.L., Mazmanian, S.K., 2009. The gut microbiota shapes intestinal immune responses during health and disease. Nat. Rev. Immunol. 9, 313.
Roy, A., Kordas, K., Lopez, P., Rosado, J.L., Cebrian, M.E., Vargas, G.G., Ronquillo, D., Stoltzfus, R.J., 2011. Association between arsenic exposure and behavior among first-graders from Torreon Mexico. Environ. Res. 111, 670–676.
Scheperjans, F., Aho, V., Pereira, P.A.B., Koskinen, K., Paulin, L., Pekkonen, E., Haapaniemi, E., Kaakkola, S., Eerola-Rautio, J., Pohja, M., et al., 2015. Gut Microbiota Are Related to Parkinson's Disease and Clinical Phenotype. Mov. Disord. 30, 350–358.
Sebastian, S.T., Sunitha, S., 2015. A cross-sectional study to assess the intelligence quotient (IQ) of school going children aged 10–12 years in villages of Mysore district, India with different fluoride levels. J. Indian Soc. Pedod. Prev. Dent. 33, 307–311.
Segata, N., Izard, J., Waldron, L., Gevers, D., Miropolsky, L., Garrett, W.S., Huttenhower, C., 2011. Metagenomic biomarker discovery and explanation. Genome Biol. 12, R60.
Thompson, T., Fawell, J., Kunikane, S., Jackson, D., Appleyard, S., Callan, P., Bartram, J., Kingston, P., 2007. World Health Organization. Water SaHT: Chemical safety of drinking water : assessing priorities for risk management.
Thursby, E., Juge, N., 2017. Introduction to the human gut microbiota. Biochem. J. 474, 1823–1836.
Tian, X., Feng, J., Dong, N., Lyu, Y., Wei, C., Li, B., Ma, Y., Xie, J., Qiu, Y., Song, G., 2019. Subchronic exposure to arsenite and fluoride from gestation to puberty induces oxidative stress and disrupts ultrastructure in the kidneys of rat offspring. Sci. Total Environ. 686, 1229–1237.
Tsai, S.Y., Chou, H.Y., The, H.W., Chen, C.M., Chen, C.J., 2003. The effects of chronic arsenic exposure from drinking water on the neurobehavioral development in adolescence. Neurotoxicology 24, 747–753.
Valles-Colomer, M., Falony, G., Darzi, Y., Tigchelaar, E.F., Wang, J., Tito, R.Y., Schiweck, C., Kurilshikov, A., Joossens, M., Wijmenga, C., 2019. The neuroactive potential of the human gut microbiota in quality of life and depression. Nat. Microbiol. 4, 623.
Vibol, S., Hashim, J.H., Sarmani, S., 2015. Neurobehavioral effects of arsenic exposure among secondary school children in the Kandal Province Cambodia. Environ. Res. 137, 329–337.
Vogt, N.M., Kerby, R.L., Dill-McFarland, K.A., Harding, S.J., Merluzzi, A.P., Johnson, S.C., Carlsson, C.M., Asthana, S., Zetterberg, H., Blennow, K., 2017. Gut microbiome alterations in Alzheimer's disease. Sci. Rep. 7, 13537.
von Ehrenstein, O.S., Poddar, S., Yuan, Y., Mazumder, D.G., Eskenazi, B., Basu, A., Hira-Smith, M., Ghosh, N., Lahiri, S., Haque, R., et al., 2007. Children's intellectual function in relation to arsenic exposure. Epidemiology 18, 44–51.
Walecki, P., Kawala-Janik, A., Siwek, J., 2018. Autism in children connected with gastrointestinal symptoms. In Gut Microbiota-Brain Axis, IntechOpen.
Wambu, E.W., Agong, S.G., Anyango, B., Akuno, W., Akenga, T., 2014. High fluoride water in Bondo-Rarieda area of Siaya County, Kenya: a hydro-geological implication on public health in the Lake Victoria Basin. BMC Publ. Health 14, 462.
Wang, S.X., Wang, Z.H., Cheng, X.T., Li, J., Sang, Z.P., Zhang, X.D., Han, L.L., Qiao, X.Y., Wu, Z.M., Wang, Z.Q., 2007. Arsenic and fluoride exposure in drinking water: children's IQ and growth in Shanyin county, Shanxi province China. Environ. Health Perspect. 115, 643–647.
Weir, T.L., Manter, D.K., Sheflin, A.M., Barnett, B.A., Heuberger, A.L., Ryan, E.P., 2013. Stool microbiome and metabolome differences between colorectal cancer patients and healthy adults. PLoS ONE 8, e70803.
Wen, D., Zhang, F., Zhang, E., Wang, C., Han, S., Zheng, Y., 2013. Arsenic, fluoride and iodine in groundwater of China. J. Geochem. Explor. 135, 1–21.
Williams, B.L., Hornig, M., Buie, T., Bauman, M.L., Paik, M.C., Wick, I., Bennett, A., Jabado, O., Hirschberg, D.L., Lipkin, W.I., 2011. Impaired carbohydrate digestion and transport and mucosal dysbiosis in the intestines of children with autism and

gastrointestinal disturbances. PLoS ONE 6, e24585.
Wu, C., Gu, X., Ge, Y., Zhang, J., Wang, J., 2006. Effects of high fluoride and arsenic on brain biochemical indexes and learning-memory in rats. Fluoride 39, 274–279.
Xu, Z., Wang, C., Dong, X., Hu, T., Wang, L., Zhao, W., Zhu, S., Li, G., Hu, Y., Gao, Q., 2019. Chronic alcohol exposure induced gut microbiota dysbiosis and its correlations with neuropsychic behaviors and brain BDNF/Gabra1 changes in mice. BioFactors 45, 187–199.
Yasuda, Koji, Hsu, Tiffany, Gallini, Carey A., Mclver, Lauren J., Schwager, Emma, Shi, Andy, DuLong, Casey R., Schwager, Randall N., Abu-Ali, Galeb S., Franzosa, Eric A., Garrett, Wendy S., Huttenhower, Curtis, Morgan, Xochitl C., Xu, Jian, 2017. Fluoride Depletes Acidogenic Taxa in Oral but Not Gut Microbial Communities in Mice. mSystems 2 (4). https://doi.org/10.1128/mSystems.00047-17.
Zhang, C., Ling, B., Liu, J., Wang, G., 1999. Effect of fluoride-arsenic exposure on the neurobehavioral development of rats offspring. *Wei sheng yan jiu* =. J. Hygiene Res. 28, 337–338.
Zheng, P., Zeng, B., Zhou, C., Liu, M., Fang, Z., Xu, X., Zeng, L., Chen, J., Fan, S., Du, X., 2016. Gut microbiome remodeling induces depressive-like behaviors through a pathway mediated by the host's metabolism. Mol. Psychiatry 21, 786–796.